UC Irvine
UC Irvine Previously Published Works

Title

Using machine learning to examine street green space types at a high spatial resolution: Application in Los Angeles County on socioeconomic disparities in exposure

Permalink

https://escholarship.org/uc/item/0w69q3pp

Journal

The Science of The Total Environment, 787(JAMA Netw. Open 2 7 2019)

ISSN

0048-9697

Authors

Sun, Yi
Wang, Xingzhi
Zhu, Jiayin
et al.

Publication Date

2021-09-01

DOI

10.1016/j.scitotenv.2021.147653

Peer reviewed

Using machine learning to examine street green space types at a high spatial resolution: Application in Los Angeles County on socioeconomic disparities in exposure

Yi Sun [a], XingzhiWang [b], Jiayin Zhu [c], Liangjian Chen [d], Yuhang Jia[e], Jean M. Lawrence [f], Luo-hua Jiang [g], Xiaohui Xie [d], JunWua,*

[a] Department of Environmental and Occupational Health, Program in Public Health, University of California, Irvine, CA, USA
[b] School of Computer Science, Beijing Institute of Technology, Beijing, China
[c] School of Management and Economics, Beijing Institute of Technology, Beijing, China
[d] Department of Computer Science, University of California, Irvine, CA, USA
[e] Testin AI Data, Beijing Yunce Information Technology Co., Ltd, China
[f] Department of Research & Evaluation, Kaiser Permanente Southern California, Pasadena, CA, USA
[g] Department of Epidemiology and Biostatistics, University of California, Irvine, CA, USA

Abstract

Background: Compared to commonly-used green space indicators from downward-facing satellite imagery, street view-based green space may capture different types of green space and represent how environments are perceived and experienced by people on the ground, which is important to elucidate the underlying mechanisms linking green space and health.
Objectives: This study aimed to evaluate machine learning models that can classify the type of vegetation (i.e., tree, low-lying vegetation, grass) from street view images; and to investigate the associations between street green space and socioeconomic (SES) factors, in Los Angeles County, California.
Methods: SES variables were obtained from the CalEnviroScreen3.0 dataset. Microsoft Bing Maps images in conjunction with deep learning were used to measure total and types of street view green space, which were compared to normalized difference vegetation index (NDVI) as commonly-used satellite-based green space measure. Generalized linear mixed model was used to examine associations between green space and census tract SES, adjusting for population density and rural/urban status.
Results: The accuracy of the deep learning model was high with 92.5% mean intersection over union. NDVI were moderately correlated with total street view-based green space and tree, and weakly correlated with low-lying vegetation and grass. Total and three types of green space showed significant negative associations with neighborhood SES. The percentage of total green space decreased by 2.62 [95% confidence interval (CI):$-3.02, -2.21$, p < 0.001] with each interquartile range increase in CalEnviroScreen3.0 score. Disadvantaged communities contained approximately 5% less average street green space than other communities.
Conclusion: Street view imagery coupled with deep learning approach can accurately and efficiently measure eye-level street green space and distinguish vegetation types. In Los Angeles County, disadvantaged communities had substantively less street green space. Governments and urban planners need to consider the type and visibility of street green space from pedestrian's perspective.

1. Introduction

Evidence that indicates inequalities in health is increasing. Researchers and policymakers have given more attention to reduce or eliminate health disparity caused by geographical locations, gender, race/ethnicity, and socioeconomic status (SES), etc. (Marmot and Bell, 2016). Inequitable access to environmental resources, such as green space, may be one of the potential explanations of socioeconomic health disparities or inequalities (World Health Organization, 2016). For example, a previous study has shown that low income neighborhoods have reduced availability of green space (Astell-Burt et al., 2014). In the U.S., race/ethnicity and poverty levels are important indicators of spatial access to green spaces (Wen et al., 2013). In addition, the green space health associations of all-cause mortality, circulatory disease, and mental well-being may be stronger among more disadvantaged groups (Astell-Burt et al., 2014; Dadvand et al., 2014; Fuertes et al., 2014; McEachan et al., 2016; Mitchell and Popham, 2007), indicating an inequitable distribution of green spaces could exacerbate health inequalities for people of lower SES, who are already at greater risk of preventable diseases. Furthermore, green spaces could lower levels of environmental hazards such as air pollution and extreme heat (Markevych et al., 2017; Sun et al., 2020a), which is also a pressing issue in the field of environmental justice.

There are various sources, scales and types of green space indicator used in epidemiological studies (Cusack et al., 2017; Klompmaker et al., 2018; Larkin and Hystad, 2019; Mitchell et al., 2011; Reid et al., 2018; Villeneuve et al., 2018). The most commonly used method to objectively assess exposure to green space is based on remote sensing data (Markevych et al., 2017; Mitchell et al., 2011), such as normalized difference vegetation index (NDVI) (Tucker, 1979) and land use or land cover databases (Helbich et al., 2018; James et al., 2015; Zock et al., 2018). However, green space from downward-facing remotely sensing imagery including NDVI and traditional land-use measures, may significantly differ from surrounding green space at the eye level. Green space from satellite data cannot fully reflect the vertical dimension of green space, especially in locations with dense greenness (Jiang et al., 2017; Li, 2018), but can better represent the horizontal dimension of green space. For example, both seen and unseen trees may improve air quality by filtering air pollutants or reducing emission sources due to the competitive land use between green space and sources of air pollution, or provide cooling benefits for their surroundings. Green space from street view images may represent how environments are perceived and experienced by people on the ground (Dong et al., 2018; Lu et al., 2018), which is critical to better understand the underlying mechanisms linking green space with human behaviors and various health outcomes. For example, eye-level street green space may be more related to mental health and physical activity (Helbich et al., 2019; Lu, 2018; Lu et al., 2018) than the overhead-view satellite assessments. According to the Stress Recovery Theory (Ulrich, 1983; Ulrich et al., 1991), natural elements (e.g. scenes, odors and sounds) activate the parasympathetic system that could decrease blood pressure, heart rate, skin conductance, and salivary cortisol level. Only eye-level, perceived and experienced green space can cause these physiological responses that could induce relaxation and help to reduce stress (Ulrich et al., 1991). Further, eyelevel street green space may promote both transportation walking and recreational walking behaviors. The evidence suggests that street green spaces improve the perceived aesthetics and quality of a neighborhood's built environment, which are key predictors of route choice and walkability (Nagata et al., 2020; Saelens and Handy, 2008; Sallis et al., 2012).

Moreover, types of green space could be efficiently recognized from high resolution street view imagery. The differences in the composition of vegetation, such as the proportion of trees and grass, might have distinctive impacts on human behavior and health through different pathways. So far, only a few epidemiological studies have investigated the effects of different types of green space (Astell-Burt and Feng, 2019; Astell-Burt and Feng, 2020; Reid et al., 2017; Zhang and Tan, 2019). Higher tree density within 1000 m was associated with better self-reported health in New York City, but not grass density (Reid et al., 2017). A study in Singapore measured urban green space in different buffer sizes between 400 m to 1600 m using three metrics: vegetation cover, canopy cover and park area. Although all three metrics were positively related to mental health, overall, canopy cover showed the strongest associations with mental health at most spatial scales (Zhang and Tan, 2019). Another study in Australia reported urban tree canopy may be a better option for promoting community mental health and preventing insufficient sleep than other urban greening (Astell-Burt and Feng, 2019; Astell-Burt and Feng, 2020). Therefore, measuring types of green space may help to better capture different aspects of green space and improve our understanding of the mechanisms that underlie green space exposure and health.

To overcome the constraints of remote sensing assessments of green space, people can use street view imagery, such as Google Street View (GSV) images to effectively characterize visual greenery along roads (Gong et al., 2018; Li, 2018; Middel et al., 2019). Street view data in combination with machine learning approach has been shown to be effective to characterize overall green space (Dong et al., 2018; Seiferling et al., 2017; Weichenthal et al., 2019). However, no prior study has applied deep learning techniques to characterize different types of green space based on high resolution street view image data. Only a few studies have applied computer vision (Larkin and Hystad, 2019; Li et al., 2015) to detect green color features or semantic segmentation techniques (Helbich et al., 2019; Lu, 2018) to measure overall green space from street view images. The types of green space were only measured using satellite imagery rather than eye-level street view data (Astell-Burt and Feng, 2020; Brandt et al., 2020). More advanced and robust deep learning architectures are needed to reliably classify types of green space based on high-resolution street view image data and thus refine the methodology and underlying pathway of health impact studies of green space.

In this study, we aimed to: 1) test and evaluate machine learning models that can reliably and efficiently classify three types of green space, i.e., tree, low-lying vegetation, and grass based on street view imagery; and 2) apply this model to examine street-level green space types and investigate their associations with socioeconomic factors in Los Angeles County, California, U.S.

2. Methods

2.1. Study population

This study was set in Los Angeles County, excluding the island areas. The primary unit of analysis was census tract (n = 2343). Los Angeles County is an ideal site to investigate the environmental justice or disparity issue related to urban greenness because it is one of the most populous (>10million people) and racially/ethnically diverse counties in the U.S. (U.S., 2015a). Minority and low-income communities in the city of Los Angeles have a high prevalence of chronic diseases and poor mental health (Brown et al., n.d.; Jennings et al., 2017; LA County,

2017; Robles et al., 2019). In terms of plant biodiversity, Los Angeles County has a particularly mild climate with high-plant species richness due to the large range of vegetation species that can thrive there (Hondagneu-Sotelo, 2014).

2.2. Socioeconomic factors

The CalEnviroScreen3.0 dataset (2018 update) was obtained from the California Communities Environmental Health Screening Tool (OEHHA, 2018). CalEnviroScreen (CES) was created and designed by the California Environmental Protection Agency (CalEPA) to address the issue of environmental justice and screening disadvantaged communities, which is suitable for community-level estimates. This tool integrates 20 indicators representing pollution and population vulnerability for all 58 counties in California. There are two main categories of indicators: pollution burden (7 exposure indicators and 5 environmental effects indicators) and population characteristics (3 sensitive population indicators and 5 socioeconomic factors). The CES Score was calculated by combining all these components (Faust et al., 2017). To comprehensively capture the population characteristics and SES for Los Angeles County at census tract-level, we included all five socioeconomic indicators (i.e., educational attainment, housing burden, linguistic isolation, poverty and unemployment), and two SES-related summary indicators (Population Characteristics Score and CalEnviroScreen3.0 Score) (Fig. 1) in this analysis. Another notable use of CES was that Senate Bill 535 requires CalEPA to identify disadvantaged communities based on geographic, socioeconomic and environmental hazard criteria. Disadvantaged community (DAC) pursuant to SB 535 (CalEPA, 2017), defined as the top 25% scoring census tracts fromCalEnviroScreen3.0,was included in this analysis as a binary variable (1038 DAC, and 1305 non-DAC in Los Angeles County). Total population and race/ethnicity data from the 2010 Census were also constructed from the CalEnviroScreen3.0 dataset.

Socioeconomic Factor Indicators (%)
- Educational Attainment (2011-2015)
- Housing Burden (2009-2013)
- Linguistic Isolation (2011-2015)
- Poverty (2011-2015)
- Unemployment (2011-2015)

Summary Indicators
- Population Characteristics Score
- CalEnviroScreen 3.0 Score

Fig. 1. Selected indicators and year of data source from CalEnviroScreen3.0. Educational Attainment: Percent of population over 25 with less than a high school education; Housing Burden: Percent housing burdened low-income households; Linguistic Isolation: Percent limited English speaking households; Poverty: Percent of population living below two times the federal poverty level; Unemployment: Percent of the population over the age of 16 that is unemployed and eligible for the labor force. Note: Full version and further information on the construction of the individual metrics is given in CalEnviroScreen3.0 Report (Faust et al., 2017).

2.3. Outcome variable: green space

2.3.1. Street view green space

We requested street view images using Microsoft Bing Maps API. Bing StreetSide provides 360-degree panoramic imagery of street-level scenes across large regions of the United States. The street network data for Los Angeles County were obtained from the U.S. Census Bureau (U.S., 2015b) and include all features within the "Road/Path Features" (e.g., primary, secondary, local neighborhood, and rural roads, city streets, alleys, bike paths or trails, etc.). Sampling points for street view images were constructed along the road network with a 200 m

space interval between each point and geocoded with ArcMap 10.5 (Esri, Redlands, CA, USA)(Li et al., 2015; Li, 2018). To include the entire streetscape, we retrieved four main cardinal directions at each point (e.g., 0, 90, 180, and 270 degrees; vertical angle: 0 degrees) (Helbich et al., 2019; Li, 2018; Lu, 2018). The amount of eye-level street green space for each point was determined by the average proportion of greenery pixels in the images of four directions. The proportion of different vegetation types in the image was predicted by the deep learning model described below. Total green space was defined as the sum of area proportion of all types of green space in each image. The size of each image was 480 × 320 pixels. To create census tract variables, all sampling points were assigned one of Los Angeles County's census tract in ArcMap. The proportion of green space for all points in a census tract were averaged to assess the census tract-level street green space, and then linked to the CalEnviroScreen3.0 data. The summary statistics of green space level and socioeconomic factors are shown in Appendix A. In the U.S., census tracts generally have a population size about 4000 inhabitants with similar population characteristics, economic status, and living conditions. In Los Angeles County, the areas of census tracts range from 0.1 to 74.5 km2 in urban area. The largest census tract in rural area has an area of 1460.5 km2. The spatial size of census tracts (5.1 ± 45.3 km2) varies widely depending on the population density. The number of sampling points (103 ± 231) per census tract varies depending on the area and street density. The distribution of street network and summary statistics of sampling points are shown in Appendix B.

2.3.2. Deep learning model and image segmentation

We applied a machine learning model using semantic segmentation to identify three different types of vegetation including tree (e.g., canopy), low-lying vegetation (e.g., shrub, bush), and grass based on high resolution street view image data.

2.3.2.1. Model structure.

Deep convolutional neural networks have achieved state-of-the-art results in semantic segmentation (Li et al., 2018). Two recent studies used classical semantic segmentation models, namely fully convolutional neural network (FCN-8 s) and Pyramid scene parsing network (PSPNet), to identify total green space from streetscape images, achieving 81.4% and 93.4% accuracy, respectively (Helbich et al., 2019; Lu, 2018).We compared top ranked semantic segmentation models on Cityscapes test in 2020 (PapersWithCode, 2020); the FCN and PSPNet models ranked 71 and 32 on the list respectively. Summary of the comparison for the top nine ranked models plus the FCN and PSPNet models are described in Appendix C. After thorough model comparison,we chose to apply a deep high-resolution representation learning model named High-Resolution Net (HRNet) coupled with the object-contextual representations (OCR)method for the classification of green space types (Wang et al., 2020; Yuan et al., 2019). The HRNet has the advantage of maintaining high-resolution representations throughout the network, making the model not only semantically strong but also spatially precise. This model can leverage multi-scale fusion mechanism, e.g., repeatedly exchange the information between high- and low-resolution subnetwork, to improve its capacity to capture both high- and low-resolution features. The OCR technique can characterize a pixel by exploiting the representation of the corresponding object class. This HRNetV2 + OCR+ model, with a high accuracy of 84.5% on Cityscapes test dataset, ranked among the top semantic segmentation models

(PapersWithCode, 2020). Appendix D illustrates the network structure of the HRNetV2 + OCR+ model.

2.3.2.2. Model training.

Annotated images from three data sources were combined to create the training and validation datasets. First, two hundred annotated images including three green space categories were obtained from ADE20K dataset, which is a densely annotated dataset covering a diverse set of scenes and object categories (Zhou et al., 2017). The existing public datasets of annotated green space images are not big enough to train and test the model. Therefore, 1000 additional Google/Tencent Street View images randomly located in southern California (N = 500)/Beijing, China (N = 500) were manually annotated using the open annotation tool "LabelMe" (Russell et al., 2008) by three researchers, and verified by a senior researcher from April 2020 to June 2020.We further increased the sample size of the training and validation data by annotating 300 street images from Cityscapes, which focuses on semantic understanding of complex urban street scenes (Cordts et al., 2016). In total, 1500 annotated images were obtained as the training and validation data for the model. Ninety percent of the annotated images were randomly selected as the training dataset and the remaining 10% as the validation dataset.

Since the proportion of images with low-lying vegetation (14.3% of images) or grass (19.1% images) was much smaller compared to that with trees (66.6% of images), we used the focal loss instead of the cross entropy in the original model to address sample imbalance (Lin et al., 2017). For the training process, we combined the focal loss function with the Adam optimizer (Kingma and Ba, 2015), which improved the model performance by 4% compared with the use of cross entropy and stochastic gradient descent (SGD) optimizer in the original model (Robbins and Monro, 1951).

We obtained image segmentations by feeding the street view images into the trained model. Then, the total number of pixels of each green space type (i.e., tree, low-lying vegetation, grass) were identified and the proportion of each type was determined (in % of pixels) for each image.

2.3.2.3. Model validation.

Intersection over union (IoU) was used to evaluate the performance of the models. Briefly, IoU is the number of overlap pixel between predicting and ground-truth divide by the union of the predicting and ground-truth, which is a common method in image segmentation field to judge the quality of predicting images (Garcia-Garcia et al., 2017).We run a 10-fold cross-validation to further evaluate the accuracy of the model (Bengio and Grandvalet, 2004). The original dataset was randomly partitioned into 10 equal-sized subsets. Of the ten subsets, one subset was retained as the validation data for testing the model, and the remaining nine subsets were used the training data. The cross-validation process was then repeated 10 times, with each of the 10 subsamples used exactly once as the validation data. Additionally, one hundred Google street view images of Los Angeles County were randomly selected as an independent test set to assess the performance of the model.

2.3.3. Normalized difference vegetation index (NDVI)

To compare the street view green space with satellite imagery-based green space, we also used the NDVI (Tucker, 1979) to characterize green space. Briefly, NDVI ranges from−1 to 1 and describes the different reflectance between visible and near-infrared wavelength of vegetation cover from satellite data, where higher values indicate more greenness. Negative values, representing water bodies, were recorded to zero before further analyses were conducted (Markevych et al., 2017), so that the effects of blue space do not negate the presence of green space. The NDVI estimates were based on the Moderate Resolution Imaging Spectroradiometer (MODIS) products from NASA. We combined measurements from both the Terra (MOD13Q1) and the Aqua (MYD13Q1) satellite instruments. The data had a spatial resolution of 250 m × 250 mand a temporal resolution of every 8-days (46 time-points annually). Because of the year-round mild-to-hot climate in Los Angeles County, green spaces do not change substantially across seasons. Previous study showed the NDVI values are highly correlated during the entire year in California (Sun et al., 2020b). Therefore, the distinction between seasons and thus the recognition of species (evergreen or deciduous species) was not taken into account. Annual average NDVI in 2015 was calculated and assigned to each census tract based on the NDVI values in all 250m grids within the census tract. In addition to the census tract-level assessment, we extracted the NDVI grid's value at the location of each sampling point along the street (N = 361,213) to examine the correlation between NDVI and street view-based green space at point level.

2.4. Statistical analyses

A GIS map was generated to show the spatial pattern of street green space across census tracts. The street green space level was calculated based on all sampling points along the road network within each census tract, and the percentage of green space for all points were averaged to assess the census tract-level street green space. The outcome variables in our analysis are four percentage of street green space (greenery pixels/total pixels) variables at a continuous scale: total and three types of green space, tree, low-lying vegetation, and grass. Percentage of green space was visualized according to their quintiles. Pearson's correlation was used to examine the correlation between green space types; t-test was applied to determine the difference between disadvantaged and other communities.

The generalized linear mixed models (GLMMs) with an identify link function and normal distribution were applied to examine the association between SES factors and street green space levels (Proc GLIMMIX in SAS). Ordinary least squares (OLS) regression was not employed because significant spatial autocorrelation was found among the residuals of OLS. Thus, we used GLMMs with spherical spatial covariance structure to account for the spatial autocorrelation in the green space outcome variables. All models included one of SES factors as the main fixed effect and adjusted for population density and rural/urban status.

The distribution of street network and spatial size vary across different census tracts (Appendix B). The sampling points in larger rural areas with sparse street network may not represent the true green space level at census tract-level due to a small number of sampling points. Therefore, we conducted sensitivity analyses restricting to only urban areas. Urban areas were defined as those with a rural-urban commuting area (RUCA) code of 1.0,which indicates

the metropolitan area core with primary flow of the population within an urbanized area (U.S., 2020) (Appendix B). All analyses were conducted with SAS 9.4 (SAS Institute, Inc., Cary, NC).

3. Results

The accuracy of our model was high with 92.5% mean IoU. The IoU values for tree, low-lying vegetation and grass were 96.2%, 86.5% and 94.4%, respectively (Appendix E). Fig. 2 shows examples of training and predicting process through the HRNetV2 + OCR+ model. The results of cross-validation were shown in Appendix F. The mean IoU in 10-fold cross-validation was 90.6% with a range of 89.4% and 91.9%, demonstrating the reliability and stability of our deep learning model. The average IoU in 10-fold cross-validation for tree, low-lying vegetation and grass were 95.4%, 84.9%, and 92.0%, respectively. Moreover, the mean IoU in the independent test set was 83.8%, and the IoU for tree, low-lying vegetation and grass were 93.7%, 71.3%, and 86.6%, respectively.
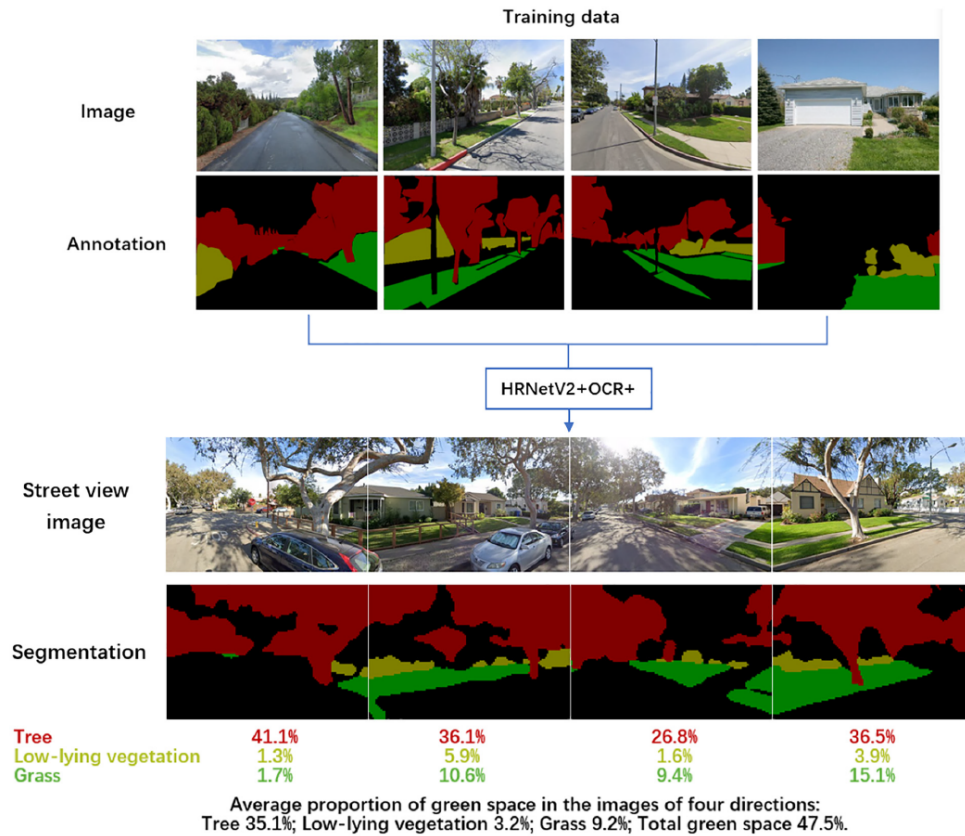

Fig. 2. Examples of green space type segmentation through HRNetV2+ OCR+.
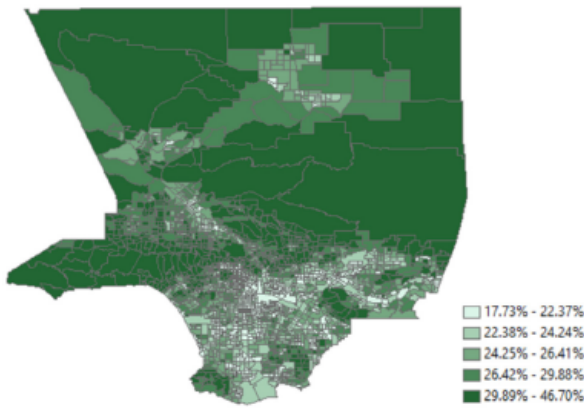
Los Angeles County population characteristics with definitions and street green space levels are presented in Table 1. Total green space and the three specific types were lower in disadvantage communities than in other communities (p<0.001). The spatial distribution of street view green space and neighborhood SES in Los Angeles County at census tract-level are depicted in Fig. 3. The map shows that total street green space had a similar spatial pattern with street tree coverage and NDVI; whereas the total green space, street tree coverage and NDVI value showed an opposite distribution pattern of CES scores.

Table 1
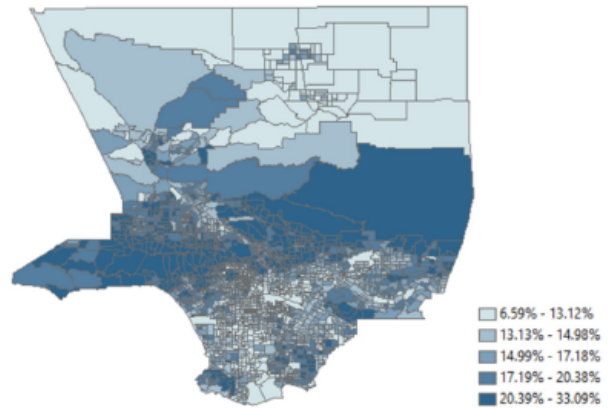Description of the population characteristics and street green space levels.

Characteristics	Disadvantaged communities n = 1038	Other communities n = 1305	Total n = 2343
CalEnviroScreen3.0 Indicators, mean (SD)			
Educational Attainment, %	38.0 (15.4)	13.3 (11.7)	24.3 (17.9)
Linguistic Isolation, %	21.4 (11.2)	9.8 (9.2)	15.0 (11.6)
Poverty, %	56.3 (15.4)	28.6 (16.3)	40.8 (21.0)
Unemployment, %	12.2 (5.0)	8.7 (3.8)	10.3 (4.7)
Housing Burden, %	29.1 (8.3)	18.6 (7.8)	23.3 (9.6)
Population Characteristics Score, 0–10	7.5 (1.0)	4.4 (1.7)	5.8 (2.1)
CalEnviroScreen3.0 Score, 0–100	51.7 (8.2)	24.3 (9.3)	36.5 (16.3)
Racial/ethnic minority groups, n (%)			
High	524 (50.5)	70 (5.4)	594 (25.3)
(4th quartile)			
Moderate/low	514 (49.5)	1235 (94.6)	1749 (74.7)
(1st–3rd quartile)			
Green space, mean (SD)			
Tree, %	14.9 (2.9)	18.4 (4.8)	16.8 (4.4)
Low-lying, %	4.2 (0.9)	4.9 (1.6)	4.6 (1.4)
Grass, %	4.6 (1.2)	5.2 (1.5)	4.9 (1.4)
Total green space, %	23.7 (2.9)	28.5 (5.1)	26.3 (4.9)
NDVI, 0–1	0.11 (0.03)	0.15 (0.04)	0.13 (0.04)

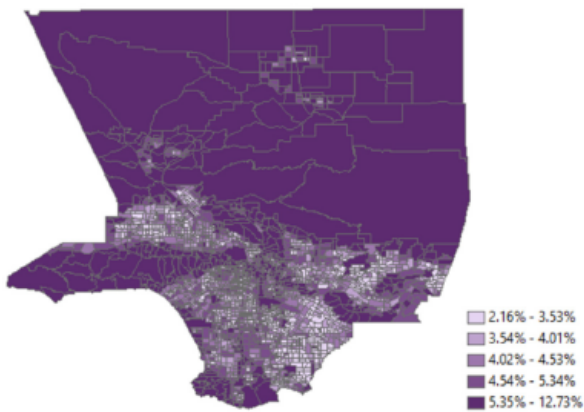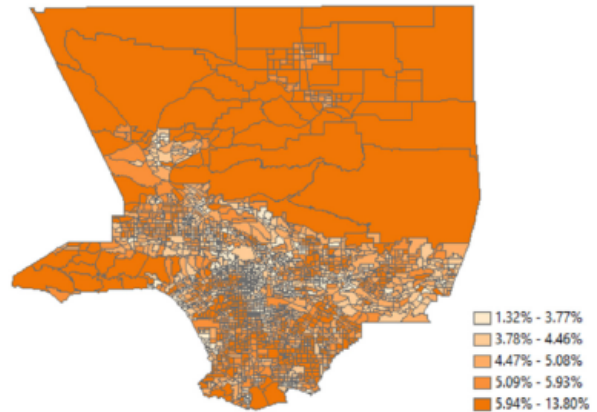SD, standard deviation. NDVI, normalized difference vegetation index.
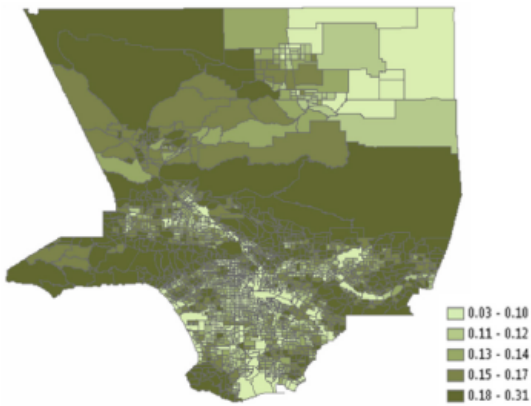
Total green space

17.73% - 22.37%
22.38% - 24.24%
24.25% - 26.41%
26.42% - 29.88%
29.89% - 46.70%

Tree

6.59% - 13.12%
13.13% - 14.98%
14.99% - 17.18%
17.19% - 20.38%
20.39% - 33.09%

Low-lying vegetation

2.16% - 3.53%
3.54% - 4.01%
4.02% - 4.53%
4.54% - 5.34%
5.35% - 12.73%

Grass

1.32% - 3.77%
3.78% - 4.46%
4.47% - 5.08%
5.09% - 5.93%
5.94% - 13.80%

NDVI

0.03 - 0.10
0.11 - 0.12
0.13 - 0.14
0.15 - 0.17
0.18 - 0.31

CalEnviroScreen Score

0.00 - 20.06
20.07 - 30.62
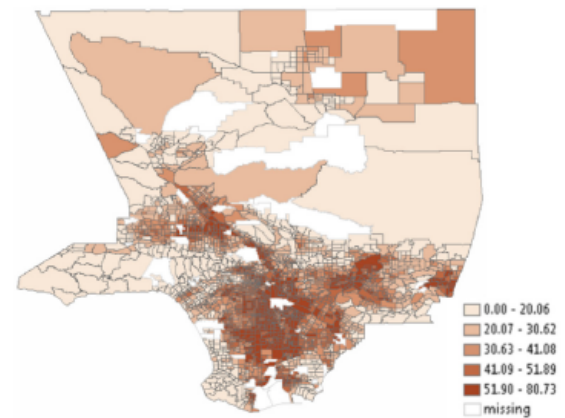30.63 - 41.08
41.09 - 51.89
51.90 - 80.73
missing

Fig. 3. Spatial pattern of street green space and neighborhood socioeconomic status in Los Angeles County, census tracts.

Table 2 shows the correlations between each type of green space from street view images and NDVI. Total tract-level green space was positively correlated with all green space types, and the correlations were most pronounced with tree (r=0.90), followed by low-lying vegetation (r=0.36) and grass (r=0.29). The correlations between street tree, low-lying vegetation and grass were weak. For NDVI, it was moderately highly correlated with total tract-level green space from street view imagery (r = 0.73). Point-level correlation between NDVI and street view green space was lower than the tract-level (r = 0.57). NDVI was moderately correlated with street tree for both point- and tract-level. However, the correlations between NDVI and low-lying vegetation and grass were weak. Moreover, green space indicators were negatively correlated with all CES socioeconomic factors. Summary statistics of green space indicators and socioeconomic factors are shown in Appendix A.

Table 2
Correlations between tract-based types of street green space, point- and census tract-based NDVI, and census tract socioeconomic factors. (Number of sampling points: 361,213; number of census tracts: 2343.)

Type	Tree	Low-lying vegetation	Grass	Total green space	Tract-NDVI	Point-NDVI	Edu-cation	Linguistic Isolation	Poverty	Unemployment	Housing Burden	Population score	CES 3.0
Tree	1.00	0.03	0.05	0.90	0.63	0.49	−0.46	−0.31	−0.44	−0.26	−0.28	−0.49	−0.45
Low-lying vegetation		1.00	0.19	0.36	0.31	0.23	−0.29	−0.26	−0.30	−0.10	−0.28	−0.34	−0.36
Grass			1.00	0.29	0.23	0.16	−0.23	−0.38	−0.28	−0.03	−0.27	−0.11	−0.21
Total green space				1.00	0.73	0.57	−0.56	−0.46	−0.56	−0.27	−0.41	−0.57	−0.57
Tract-NDVI					1.00	1.00	−0.55	−0.53	−0.63	−0.29	−0.52	−0.59	−0.59

Table 3 shows the results of the GLMMs to assess the association of street green space with neighborhood SES, controlling for population density and urban/rural status. Overall, we found statistically significant inverse associations between SES factors and street green space. For example, for each interquartile range (IQR) increase in CES score (26 unit), the percentage of total green space decreased by 2.62 (95% CI:−3.02 to −2.21, p<0.001). The percentage of total green space in disadvantaged communities was 1.26 less than in other communities, accounting for approximately 5% of average street green space in Los Angeles County.

A similar trend was observed in sensitivity analyses by restricting to urban areas. In addition, associations between socioeconomic factors and street green space were slightly stronger after restricting to urban areas (Appendix G).

Table 3
Associations between neighborhood socioeconomic status and green space in Los Angeles County, census tracts.

Socioeconomic status	IQR[a]	Tree		Low-lying vegetation		Grass		Total green space		NDVI[c]	
		Regression coefficient	95% CI[b]	Regression coefficient	95% CI	Regression coefficient	95% CI	Regression coefficient	95% CI	Regression coefficient	95% CI
CalEnviroScreen 3.0 Score, 0–100	26.0	−2.26	(−2.64, −1.88)	0.07	(−0.05, 0.19)	−0.42	(−0.55, −0.30)	−2.62	(−3.02, −2.21)	−0.022	(−0.026, −0.019)
Population Characteristics Score, 0–10	3.3	−1.89	(−2.27, −1.52)	−0.18	(−0.30, −0.07)	−0.46	(−0.59, −0.34)	−2.54	(−2.94, −2.15)	−0.019	(−0.022, −0.015)
Educational Attainment, %	30.2	−1.81	(−2.20, −1.42)	−0.08	(−0.20, 0.04)	−0.44	(−0.57, −0.31)	−2.33	(−2.74, −1.92)	−0.014	(−0.018, −0.011)
Linguistic Isolation, %	15.7	−0.78	(−1.02, −0.54)	−0.03	(−0.10, 0.04)	−0.25	(−0.33, −0.17)	−1.06	(−1.32, −0.80)	−0.010	(−0.012, −0.007)
Poverty, %	35.9	−1.87	(−2.20, −1.54)	−0.03	(−0.14, 0.07)	−0.51	(−0.62, −0.40)	−2.41	(−2.76, −2.07)	−0.018	(−0.020, −0.015)
Unemployment, %	5.6	−0.29	(−0.30, −0.01)	0	(−0.04, 0.05)	−0.01	(−0.06, 0.04)	−0.16	(−0.32, −0.01)	−0.001	(−0.002, 0.000)
Housing Burden, %	13.6	−0.60	(−0.81, −0.39)	−0.01	(−0.08, 0.05)	−0.21	(−0.28, −0.14)	−0.82	(−1.04, −0.60)	−0.006	(−0.008, −0.004)
Disadvantaged community, yes	–	−0.97	(−1.29, −0.66)	−0.01	(−0.11, 0.08)	−0.27	(−0.38, −0.17)	−1.26	(−1.59, −0.93)	−0.010	(−0.013, −0.007)
Racial/ethnic minority groups, high	–	−0.92	(−1.32, −0.51)	−0.11	(−0.23, 0.02)	−0.23	(−0.36, −0.10)	−1.25	(−1.68, −0.82)	−0.006	(−0.010, −0.003)

All models were adjusted for population density and urban/rural status.
[a] IQR, interquartile range.
[b] CI, confidence interval.
[c] NDVI, normalized difference vegetation index.

4. Discussion

To the best of our knowledge, this is the first study to examine different types of green space using street view images in combination with deep learning techniques. The results from this study suggest that Bing StreetSide images are valuable sources and machine learning techniques are powerful tools to measure overall and types of street green space. In this analysis, street view-based green spaces were inequitably distributed in populations with different neighborhood SES in Los Angeles County, the most populous county in the U.S. We found that communities with a higher percentage of low SES and higher percentage of residents from racial/ethnic minority groups had substantively less street green space availability.

The fact that low-income neighborhoods have less green space is well established (Astell-Burt et al., 2014; Dai, 2011; Wen et al., 2013; Wolch et al., 2014). Several studies have revealed that the distribution of urban green space often disproportionately benefits predominantly non-Hispanic White and more affluent communities. However, most previous studies used geographic information system-based methods to measure green space from an overhead view (e.g., satellite data). Our results support the previous findings by measuring eye-level street view-based green space, suggesting that populations who have higher prevalence of poor health outcomes (Shaw, 2016) live in environments that contain the least green space for supporting positive lifestyle modification. Furthermore, our results showed that the magnitude of association between green space and neighborhood SES varied between vegetation types. The greatest reduction was observed among the tree, followed by grass. However, we observed inconsistent associations of low-lying vegetation and neighborhood SES, which warrants further research. In addition, the relative associations of lower SES with NDVI are greater than total street green space, suggesting that deprived communities may contain additionally reduced "unseen" green space, such as private green spaces or large areas of park, forest away from the road.

Street view data and deep learning techniques are increasingly used for environmental exposure assessments for health-related studies. Previous studies have suggested that walking behavior and physical activity is affected by eye-level street green space (Lu, 2018; Villeneuve et al., 2018). For example, a study in Canada compared the NDVI with the google street viewmeasure of green space, and found that only street green space was positively associated with participation in recreational physical activities (Villeneuve et al., 2018). In addition, contact with surrounding green space might be more important if green space has the greater influence on health via restorative properties and stress reduction (Mitchell et al., 2011). For instance, street view green spaces were protective against depression for the elderly in China, whereas no significant associations were found with satellite-based green space estimates (Helbich et al., 2019). Two previous studies used the FCN-8 s and PSPNet models to identify total green space from street view images with moderate to excellent performance (81.4% and 93.4% accuracy, respectively) (Helbich et al., 2019; Lu, 2018). However, no prior study has applied street view data in conjunction with deep learning approach to classify vegetation types. Measuring types of green space is important to better understand the mechanisms linking green space to health and design urban planning interventions. Different vegetation types shown different capacity to provide the ecosystems services of air purification and microclimate regulation (Vieira et al., 2018). In addition, green space types can affect human behaviors. For example, more proportions of walking and running people were observed on the lawn and in the shade of trees than in other

settings (Wang et al., 2019). Investigating their different roles may contribute to better understanding of etiological mechanisms and the ability to design targeted interventions. Existing studies regarding different types of green space and health are sparse and mainly focused on tree canopy. Two recent studies measured green space using machine learning and image classification processes across satellite imagery (Astell-Burt and Feng, 2020; Brandt et al., 2020). However, grass and low-lying vegetation were likely under-estimated in areas where they were beneath tree canopy. Our model overcomes the limitations of existing green space metrics and contributes to the improvement of green space exposure assessment methodology for health studies. Future studies are warranted to investigate the relationships between types of green space and other environmental factors and health outcomes using this deep learning technique.

Previous studies observed poor correlation between street view-based green space and satellite-derived NDVI (Helbich et al., 2019; Larkin and Hystad, 2019; Villeneuve et al., 2018). In our correlation analyses, we observed that both community-level and point-level street view-based total green space were moderately correlated with NDVI. The differences in the climate and vegetation density in the study area may partially explain the variation in results compare to the literature. First, green spaces did not change substantially across seasons due to the year-round mild-to-hot climate in Los Angeles County. The NDVI values are highly correlated during the entire year in California (Sun et al., 2020b). However, the variation of NDVI and street view green space in Los Angeles County might not represent green space levels in other geographical settings, such as Beijing, China (Helbich et al., 2019), and Ottawa, Canada (Villeneuve et al., 2018) with four distinct seasons. Second, the overhead-view assessments cannot fully capture the vertical dimension of green space, especially in locations with high-density vegetation (Jiang et al., 2017; Li et al., 2018). The substantially lower NDVI in Los Angeles County suggested it has thinner greenness than other study regions, such as Portland and Ottawa (Larkin and Hystad, 2019; Villeneuve et al., 2018). Thus, the NDVI may be more highly correlated with overall street green space in Los Angeles County than those in previous research. Moreover, the NDVI captures both public and private (e.g., residential backyard or gated community) green spaces, while the street view imagery mainly captures publicly accessible street-based green spaces that may be most relevant to people's daily activity patterns, such as walking, jogging/running, and driving. Los Angeles metropolitan area has the nation's densest road network (road length≈55,785 km) (Sorensen, 2009). Therefore, we may expect the denser street network, the higher correlations between NDVI and street view green space. Indeed, we found the correlation coefficient for urban census tracts (r = 0.77) with denser streets was higher than rural census tracts (r = 0.54) in this study. Furthermore, the method of extracting green space and the density of street networks might be potential explanations of the differences between point-level and tract-level correlations. The point-level variations can be caused by the different perspective and spatial resolution between NDVI and street view green space. The street view-based estimate represents the horizontal panoramic 360 degrees view of each sampling point along the road thus localized green space at the particular point; while the NDVI-based estimate reflects the bird's eye view green space within a grid with cell size 250m× 250m. The street view sampling points are likely not in the center of satellite-based NDVI grids. The tract-level green space that contains multiple points or grids may smooth out the local variations and spatial mismatch in point vs. grid measurements, thus we observed higher correlation (r = 0.73) between tract-level street view green space and NDVI, both of which reflect overall community green space level, especially for urban areas with high-density roads. It is also noteworthy that tree canopy is what

people see the most for the total green space (64%) at the horizontal level. The correlation is only 0.49 for point-based NDVI and tree, indicating that vertical NDVI may not be a good indicator of horizontal tree canopy at a local level. In addition, correlations between NDVI and low-lying vegetation or grass were weak, indicating that the street view-based metrics capture additional information of visible street green space. Street view and satellite data reflect different aspects of natural environments. Green space assessments combining remote-sensing imagery and street view imagery may therefore represent more comprehensive characteristics of green space than assessments based on a single green space indicator (Larkin and Hystad, 2019), and provide a potential new approach to examine green space in epidemiological research.

The main strengths of our study include the diversity of the types of street view-based green space as well as the diversity of race/ethnic composition and SES of the population in Los Angeles County; the comparison with the predominant, satellite-based green space indicator - NDVI; the use of Bing Maps data that are publicly available and provides high-resolution images with mostly full coverage in the U.S.; the robust performance and application of an advanced deep learning model; and the generalizability of this deep learning approach in other regions in the future.

However, this study has limitations, which suggest avenues for further research. First, street view images from Bing Maps were captured in different years and dates thus this database is most suitable for long-term estimation rather than seasonal or higher temporal resolution measurement. Nevertheless, given the year-round mild and dry climate in LA, the temporal variation of green space in urban areas tends to be small. Moreover, the training data directly impact the quality of the prediction. This model was trained mainly based on the street view images from southern California. Further evaluation of the model is warranted when the model applies to other regions with different streetscapes or landforms. Additionally, a single-round annotation was used in this study. Future studies may perform double annotation (i.e., a second round of annotation) to minimize the misclassification. Next, more sophisticated subtypes of green space were not examined in this research. Future studies may take into account other vegetation types (e.g., flowers), and quality of green space (e.g., wild vegetation vs. cultivated and well-maintained vegetation). Further, because the sampling points were extracted along the road, and the density and pattern of street networks could vary across different regions. Thus, the study findings need to be interpreted with caution, particularly in large rural areas. Nonetheless, the street level images, even though having sparse road network in rural areas, still represent publicly available eyelevel green space. The "private" or not accessible greenery in both rural and urban areas may have less impact on human behaviors due to the lack of accessibility. In addition to the amount of green space, perceived quality and accessibility of green space may play an important role, because they could affect the use of green space (de la Barrera et al., 2016; Zhang et al., 2017). Further research is needed considering more information on the use of green space and individual activity patterns, especially for epidemiological studies linking green space to health outcomes.

This study provides a unique understanding of the relationship between green space and neighborhood SES. Compared to remote sensing data, street view data reflect different aspects of natural environments. Street view images coupled with deep learning approach can accurately and efficiently extract street green space and recognize different vegetation types, which can contribute to methodological development and mechanistic understanding of green space-related health studies. Results from this study indicate that green spaces were inequitably distributed in populations with different SES in Los Angeles County. Communities with a higher percentage of

low SES and racial/ethnic minority communities had substantively lower street green space level. Governments and urban planners may consider not only the size or density of green space, but also the type and visibility of street green space from pedestrian's perspective.

CRediT authorship contribution statement

Yi Sun: Formal analysis, Data curation, Software, Investigation, Methodology, Project administration, Visualization, Writing – original draft.

Xingzhi Wang: Software, Formal analysis, Validation, Visualization, Writing – review & editing.

Jiayin Zhu: Software, Formal analysis, Validation, Visualization, Writing – review & editing.

Liangjian Chen: Software, Methodology, Writing – review & editing.

Yuhang Jia: Investigation, Software.

Jean M. Lawrence: Funding acquisition, Writing – review & editing.

Luo-hua Jiang: Software, Methodology, Writing – review & editing.

Xiaohui Xie: Methodology, Resources, Software, Project administration, Writing – review & editing.

Jun Wu: Conceptualization, Data curation, Funding acquisition, Methodology, Project administration, Resources, Supervision, Writing – review & editing.

Declaration of competing interest

The authors declare that they have no known competing financial interests or personal relationships that could have appeared to influence the work reported in this paper.

Acknowledgement

Supplementary data

Supplementary data to this article can be found online at https://doi.org/10.1016/j.scitotenv.2021.147653.

References

Astell-Burt, T., Feng, X., 2019. Association of Urban Green Space With Mental Health and General Health Among Adults in Australia. JAMA Netw. Open 2 (7), e198209. https:// doi.org/10.1001/jamanetworkopen.2019.8209.

Astell-Burt, T., Feng, X., 2020. Does sleep grow on trees? A longitudinal study to investigate potential prevention of insufficient sleep with different types of urban green space. SSM Popul. Health 10, 100497. https://doi.org/10.1016/j.ssmph.2019.100497.

Astell-Burt, T., Feng, X., Mavoa, S., Badland, H.M., Giles-Corti, B., 2014. Do low-income neighbourhoods have the least green space? A cross-sectional study of Australia's most populous cities. BMC Public Health 14 (1), 292. https://doi.org/10.1186/1471-2458-14-292.

de la Barrera, F., Reyes-Paecke, S., Banzhaf, E., 2016. Indicators for green spaces in contrasting urban settings. Ecol. Indic. 62, 212–219. https://doi.org/10.1016/j.ecolind.2015.10.027.

Bengio, Y., Grandvalet, Y., 2004. No unbiased estimator of the variance of k-fold Cross-validation. J. Mach. Learn. Res. 5, 1089–1105.

Brandt, M., Tucker, C.J., Kariryaa, A., Rasmussen, K., Abel, C., Small, J., ... Fensholt, R., 2020. An unexpectedly large count of trees in the West African Sahara and Sahel. Nature 587 (7832), 78–82. https://doi.org/10.1038/s41586-020-2824-5.

Brown, P. M., Gonzalez M Fau - Dhaul, R. S., & Dhaul, R. S. Cost of chronic disease in California: estimates at the county level. (1550–5022 (Electronic)).

CalEPA, 2017. Designation of Disadvantaged Communities Pursuant to Senate Bill 535 (de León). California Environmental Protection Agency https://calepa.ca.gov/wp-content/uploads/sites/6/2017/04/SB-535-Designation-Final.pdf.

Cheng, B., Collins, M., Zhu, Y., Liu, T., Huang, T., Adam, H., Chen, L., 2020. Panoptic-DeepLab: a simple, strong, and fast baseline for bottom-up panoptic segmentation. arXiv:1911.10194v3.

Cordts, M., Omran, M., Ramos, S., Rehfeld, T., Enzweiler, M., Benenson, R., ... Schiele, B., 2016. The cityscapes dataset for semantic urban scene understanding. Computer Vision and Pattern Recognition (CVPR).

Cusack, L., Larkin, A., Carozza, S.E., Hystad, P., 2017. Associations between multiple green spacemeasures and birthweight across two US cities. Health Place 47, 36–43. https://doi.org/10.1016/j.healthplace.2017.07.002.

Dadvand, P., Wright, J., Martinez, D., Basagana, X., McEachan, R.R., Cirach, M., ... Nieuwenhuijsen, M.J., 2014. Inequality, green spaces, and pregnant women: roles of ethnicity and individual and neighbourhood socioeconomic status. Environ. Int. 71, 101–108. https://doi.org/10.1016/j.envint.2014.06.010.

Dai, D., 2011. Racial/ethnic and socioeconomic disparities in urban green space accessibility: where to intervene? Landsc. Urban Plan. 102 (4), 234–244. https://doi.org/10.1016/j.landurbplan.2011.05.002.

Dong, R., Zhang, Y., Zhao, J., 2018. How green are the streets within the sixth ring road of Beijing? An analysis based on Tencent street view pictures and the green view index. Int. J. Environ. Res. Public Health 15 (7). https://doi.org/10.3390/ijerph15071367.

Faust, J., August, L., Bangia, K., Galaviz, V., Leichty, J., Prasad, S., ... Zeise, L., 2017. CalEnviroScreen 3.0. California Environmental Protection Agency and Environmental Health Hazard Assessment https://oehha.ca.gov/media/downloads/calenviroscreen/report/

ces3report.pdf.

Fuertes, E., Markevych, I., von Berg, A., Bauer, C.P., Berdel, D., Koletzko, S., ... Heinrich, J., 2014. Greenness and allergies: evidence of differential associations in two areas in Germany. J. Epidemiol. Community Health 68 (8), 787–790. https://doi.org/10.1136/jech-2014-203903.

Garcia-Garcia, A., Orts-Escolano, S., Oprea, S., VillenaMartinez, V., Garcia-Rodriguez, J., 2017. A review on deep learning techniques applied to semantic segmentation. arXiv: 1704.06857.

Gong, F.-Y., Zeng, Z.-C., Zhang, F., Li, X., Ng, E., Norford, L.K., 2018. Mapping sky, tree, and building view factors of street canyons in a high-density urban environment. Build. Environ. 134, 155–167. https://doi.org/10.1016/j.buildenv.2018.02.042.

Helbich, M., Klein, N., Roberts, H., Hagedoorn, P., Groenewegen, P.P., 2018. More green space is related to less antidepressant prescription rates in the Netherlands: a Bayesian geoadditive quantile regression approach. Environ. Res. 166, 290–297. https://doi.org/10.1016/j.envres.2018.06.010.

Helbich, M., Yao, Y., Liu, Y., Zhang, J., Liu, P., Wang, R., 2019. Using deep learning to examine street view green and blue spaces and their associations with geriatric depression in Beijing, China. Environ. Int. 126, 107–117. https://doi.org/10.1016/j.envint.2019.02.013.

Hondagneu-Sotelo, P., 2014. Paradise Transplanted: Migration and the Making of California Gardens. University of California Press, Oakland, CA.

James, P., Banay, R.F., Hart, J.E., Laden, F., 2015. A review of the health benefits of greenness. Curr. Epidemiol. Rep. 2 (2), 131–142. https://doi.org/10.1007/s40471-015-0043-7.

Jennings, V., Baptiste, A.K., Osborne Jelks, N., Skeete, R., 2017. Urban green space and the pursuit of health equity in parts of the United States. Int. J. Environ. Res. Public Health 14 (11). https://doi.org/10.3390/ijerph14111432.

Jiang, B., Deal, B., Pan, H., Larsen, L., Hsieh, C.-H., Chang, C.-Y., Sullivan, W.C., 2017. Remotely-sensed imagery vs. eye-level photography: evaluating associations among measurements of tree cover density. Landsc. Urban Plan. 157, 270–281. https://doi.org/10.1016/j.landurbplan.2016.07.010.

Kingma, D.P., Ba, J., 2015. Adam: A method for stochastic optimization. 3rd International Conference for Learning Representations, San Diego.

Klompmaker, J.O., Hoek, G., Bloemsma, L.D., Gehring, U., Strak, M., Wijga, A.H., ... Janssen, N.A.H., 2018. Green space definition affects associations of green space with overweight and physical activity. Environ. Res. 160, 531–540. https://doi.org/10.1016/j.envres.2017.10.027.

LA County, 2017. Los Angeles County Department of Public Health. Key Indicators of Health by Service Planning Area. http://publichealth.lacounty.gov/ha/docs/2015LACHS/KeyIndicator/PH-KIH_2017-sec%20UPDATED.pdf.

Larkin, A., Hystad, P., 2019. Evaluating street view exposure measures of visible green space for health research. J. Expo. Sci. Environ. Epidemiol. 29 (4), 447–456. https://doi.org/10.1038/s41370-018-0017-1.

Li, B., Shi, Y., Qi, Z., Chen, Z., 2018. A Survey on Semantic Segmentation. pp. 1233–1240 https://doi.org/10.1109/icdmw.2018.00176.

Li, X., Zhang, C., Li, W., Ricard, R., Meng, Q., Zhang, W., 2015. Assessing street-level urban greenery using Google Street View and a modified green view index. Urban For.

Urban Green. 14 (3), 675–685. https://doi.org/10.1016/j.ufug.2015.06.006.

Li, X., Zhang, L., You, A., Yang, M., Yang, K., Tong, Y., 2019. Global aggregation then local distribution in fully convolutional networks. arXiv:1909.07229v1.

Li, X.J., 2018. GitHub. https://github.com/xiaojianggis/Treepedia_Public.

Lin, T.-Y., Goyal, P., Girshick, R., He, K., Dollar, P., 2017. Focal loss for dense object detection. Proceedings of the IEEE International Conference on Computer Vision (ICCV), pp. 2980–2988.

Lu, Y., 2018. The Association of Urban Greenness and Walking Behavior: using Google street view and deep learning techniques to estimate residents' exposure to urban greenness. Int. J. Environ. Res. Public Health 15 (8). https://doi.org/10.3390/ijerph15081576.

Lu, Y., Sarkar, C., Xiao, Y., 2018. The effect of street-level greenery on walking behavior: evidence from Hong Kong. Soc. Sci. Med. 208, 41–49. https://doi.org/10.1016/j.socscimed.2018.05.022.

Markevych, I., Schoierer, J., Hartig, T., Chudnovsky, A., Hystad, P., Dzhambov, A.M., al., e., 2017. Exploring pathways linking greenspace to health: theoretical and methodological guidance. Environ. Res. 158, 301–317.

Marmot,M., Bell, R., 2016. Social inequalities in health: a proper concern of epidemiology. Ann. Epidemiol. 26 (4), 238–240.

McEachan, R.R., Prady, S.L., Smith, G., Fairley, L., Cabieses, B., Gidlow, C., ... Nieuwenhuijsen, M.J., 2016. The association between green space and depressive symptoms in pregnant women: moderating roles of socioeconomic status and physical activity. J. Epidemiol. Community Health 70 (3), 253–259. https://doi.org/10.1136/jech-2015-205954.

Middel, A., Lukasczyk, J., Zakrzewski, S., Arnold, M., Maciejewski, R., 2019. Urban form and composition of street canyons: a human-centric big data and deep learning approach. Landsc. Urban Plan. 183, 122–132. https://doi.org/10.1016/j.landurbplan.2018.12.001.

Mitchell, R., Popham, F., 2007. Greenspace, urbanity and health: relationships in England. J. Epidemiol. Community Health 61 (8), 681–683. https://doi.org/10.1136/jech.2006.053553.

Mitchell, R., Astell-Burt, T., Richardson, E.A., 2011. A comparison of green space indicators for epidemiological research. J. Epidemiol. Community Health 65 (10), 853–858. https://doi.org/10.1136/jech.2010.119172.

Mohan, R., Valada, A., 2020. EfficientPS: efficient panoptic segmentation. arXiv:2004.02307v2.

Nagata, S., Nakaya, T., Hanibuchi, T., Amagasa, S., Kikuchi, H., Inoue, S., 2020. Objective scoring of streetscape walkability related to leisure walking: statistical modeling approach with semantic segmentation of Google Street View images. Health Place 66, 102428. https://doi.org/10.1016/j.healthplace.2020.102428.

OEHHA, 2018. CalEnviroScreen 3.0. The Office of Environmental Health Hazard Assessment, and the California Environmental Protection Agency https://oehha.ca.gov/calenviroscreen/maps-data/download-data.

PapersWithCode, 2020. https://paperswithcode.com/sota/semantic-segmentation-oncityscapes. Reid, C.E., Clougherty, J.E., Shmool, J.L.C., Kubzansky, L.D., 2017. Is all urban green space the same? A comparison of the health benefits of trees and grass in New York City. Int. J. Environ. Res. Public Health 14 (11). https://doi.org/10.3390/ijerph14111411.

Reid, C.E., Kubzansky, L.D., Li, J., Shmool, J.L., Clougherty, J.E., 2018. It's not easy assessing greenness: a comparison of NDVI datasets and neighborhood types and their associations with self-rated health in New York City. Health Place 54, 92–101. https://doi.org/10.1016/j.healthplace.2018.09.005.

Robbins, H., Monro, S., 1951. A stochastic approximation method. Ann. Math. Stat. 400–407.

Robles, B., Thomas, C., Lai, E.S., Kuo, T., 2019. A geospatial analysis of health,mental health, and stressful community contexts in Los Angeles County. Prev. Chronic Dis. 16, 190138 doi:10.5888/.

Russell, B., Torralba, A., Murphy, K., Freeman, W.T., 2008. LabelMe: a database and web-based tool for image annotation. Int. J. Comput. Vis. 77 (1-3), 157–173. https://doi.org/10.1007/s11263-007-0090-8.

Saelens, B.E., Handy, S.L., 2008. Built environment correlates of walking: a review. Med. Sci. Sports Exerc. 40 (7 SUPPL.1), S550–S566. https://doi.org/10.1249/MSS.0b013e31817c67a4.

Sallis, J.F., Floyd, M.F., Rodriguez, D.A., Saelens, B.E., 2012. Role of built environments in physical activity, obesity, and cardiovascular disease. Circulation 125 (5), 729–737. https://doi.org/10.1161/CIRCULATIONAHA.110.969022.

Seiferling, I., Naik, N., Ratti, C., Proulx, R., 2017. Green streets − quantifying and mapping urban trees with street-level imagery and computer vision. Landsc. Urban Plan. 165, 93–101. https://doi.org/10.1016/j.landurbplan.2017.05.010.

Shaw, K.M., 2016. Chronic disease disparities by county economic status and metropolitan classification, Behavioral Risk Factor Surveillance System, 2013. Prev. Chronic Dis. 13.

Shelhamer, E., Long, J., Darrell, T., 2016. Fully convolutional networks for semantic segmentation.arXiv:1605.06211v1.

Sorensen, P., 2009. Moving Los Angeles. ACCESS Mag. 1 (35), 16–24.

Sun, Y., Ilango, S.D., Schwarz, L., Wang, Q., Chen, J.C., Lawrence, J.M., ... Benmarhnia, T., 2020a. Examining the joint effects of heatwaves, air pollution, and green space on the risk of preterm birth in California. Environ. Res. Lett. 15 (10), 104099. https://doi.org/10.1088/1748-9326/abb8a3.

Sun, Y., Sheridan, P., Laurent, O., Li, J., Sacks, D.A., Fischer, H., ... Wu, J., 2020b. Associations between green space and preterm birth: windows of susceptibility and interaction with air pollution. Environ. Int. 142, 105804. https://doi.org/10.1016/j.envint.2020.105804.

Tucker, C.J., 1979. Red and photographic infrared linear combinations for monitoring vegetation. Remote Sens. Environ. 8 (2), 127–150.

U.S., 2015a. Census Bureau. New Census Bureau population estimates reveal metro areas and counties that propelled growth in Florida and the nation. https://www.census.gov/newsroom/press-releases/2015/cb15-56.html.

U.S., 2015b. Census Bureau. TIGER/Line Shapefile, Los Angeles County, CA, All Roads County-based Shapefile. https://catalog.data.gov/dataset/tiger-line-shapefile-2015-county-los-angeles-county-ca-all-roads-county-based-shapefile.

U.S., 2020. United States Department of Agriculture. 2010 Rural Urban Commuting Area (RUCA) Codes. Available at:. https://www.ers.usda.gov/data-products/rural-urbancommuting-area-codes.aspx. (Accessed August 2020).

Ulrich, R.S., 1983. Aesthetic and affective response to natural environment. Human Behavior

& Environment: Advances in Theory & Research. 6, pp. 85–125. https://doi.org/10.1007/978-1-4613-3539-9_4.

Ulrich, R.S., Simons, R.F., Losito, B.D., Fiorito, E., Miles, M.A., Zelson, M.S., 1991. Stress Recovery during exposure to natural and urban environments. J. Environ. Psychol. 11, 201–230.

Vieira, J., Matos, P.,Mexia, T., Silva, P., Lopes, N., Freitas, C., ... Pinho, P., 2018. Green spaces are not all the same for the provision of air purification and climate regulation services: the case of urban parks. Environ. Res. 160, 306–313. https://doi.org/10.1016/j.envres.2017.10.006.

Villeneuve, P.J., Ysseldyk, R.L., Root, A., Ambrose, S., DiMuzio, J., Kumar, N., ... Rainham, D., 2018. Comparing the normalized difference vegetation index with the Google street view measure of vegetation to assess associations between greenness, walkability, recreational physical activity, and health in Ottawa, Canada. Int. J. Environ. Res. Public Health 15 (8). https://doi.org/10.3390/ijerph15081719.

Wang, H., Dai, X.,Wu, J.,Wu, X., Nie, X., 2019. Influence of urban green open space on residents' physical activity in China. BMC Public Health 19 (1), 1093. https://doi.org/10.1186/s12889-019-7416-7.

Wang, J., Sun, K., Cheng, T., Cheng, T., Jiang, B., Deng, C., ... Xiao, B., 2020. Deep high-resolution representation learning for visual recognition. IEEE Trans. Pattern Anal. Mach. Intell. https://doi.org/10.1109/tpami.2020.2983686.

Weichenthal, S., Hatzopoulou,M., Brauer,M., 2019. A picture tells a thousand...exposures: opportunities and challenges of deep learning image analyses in exposure science and environmental epidemiology. Environ. Int. 122, 3–10. https://doi.org/10.1016/j.envint.2018.11.042.

Wen, M., Zhang, X., Harris, C.D., Holt, J.B., Croft, J.B., 2013. Spatial disparities in the Distribution of parks and green spaces in the USA. Ann. Behav. Med. 45 (Suppl. 1), S18–S27. https://doi.org/10.1007/s12160-012-9426-x.

Wolch, J.R., Byrne, J., Newell, J.P., 2014. Urban green space, public health, and environmental justice: the challenge of making cities 'just green enough'. Landsc. Urban Plan. 125, 234–244. https://doi.org/10.1016/j.landurbplan.2014.01.017.

World Health Organization, Urban Green Spaces and Health. A Reviewof Evidence http://www.euro.who.int/__data/assets/pdf_file/0005/321971/Urban-green-spaces-andhealth-review-evidence.pdf?ua=1.

Yuan, Y., Chen, X., Wang, J., 2019. Object-contextual representations for semantic segmentation. arXiv: 1909.11065.

Zhang, H., Wu, C., Zhang, Z., Zhu, Y., Lin, H., Zhang, Z., ... Smola, A., 2020a. ResNeSt: split-Attention networks. arXiv:2004.08955v1.

Zhang, L., Tan, Y., 2019. Associations between urban green spaces and health are dependent on the analytical scale and how urban green spaces are measured. Int. J. Environ. Res. Public Health 16 (4). https://doi.org/10.3390/ijerph16040578.

Zhang, X., Xu, H.,Mo, H., Tan, J., Yang, C., Ren,W., 2020b. DCNAS: densely connected neural architecture search for semantic image segmentation. arXiv:2003.11883v1.

Zhang, Y., Van den Berg, A.E., Van Dijk, T., Weitkamp, G., 2017. Quality over quantity: Contribution of urban green space to neighborhood satisfaction. Int. J. Environ. Res. Public Health 14 (5). https://doi.org/10.3390/ijerph14050535.

Zhao, H., Shi, J., Qi, X., Wang, X., Jia, J., 2017. Pyramid scene parsing network. arXiv:

1612.01105v2.

Zhou, B., Zhao, H., Puig, X., Fidler, S., Barriuso, A., Torralba, A., 2017. Scene parsing through ADE20K dataset. Computer Vision and Pattern Recognition (CVPR).

Zhu, Y., Sapra, K., Reda, F., Shih, K.,Newsam, S., Tao, A., Catanzaro, B., 2019. Improving semantic segmentation via video propagation and label relaxation. arXiv:1812.01593v3.

Zock, J.P., Verheij, R., Helbich,M., Volker, B., Spreeuwenberg, P., Strak,M., ... Groenewegen, P., 2018. The impact of social capital, land use, air pollution and noise on individual morbidity in Dutch neighbourhoods. Environ. Int. 121 (Pt 1), 453–460. https://doi.org/10.1016/j.envint.2018.09.008.

* Corresponding author at: Anteater Instruction & Research Bldg, 2034, 653 East Peltason Drive, University of California, Irvine, CA 92697-3957, USA.
E-mail address: junwu@hs.uci.edu (J.Wu).